CONF-7609127--1

LA-UR -77-550

TITLE: AN INVESTIGATION OF CREEP INSTABILITY AS A MECHANISM FOR GLACIER SURGES

AUTHOR(S): W.S.B. Paterson
U. Nitsan
G.K.C. Clarke

SUBMITTED TO: Proceedings of the International Workshop on the Dynamics of Glacier Variations and Surges, Alma Ata, USSR, September 1976. Will be published in English and Russian by the Academy of Sciences of the USSR.

los alamos
scientific laboratory
of the University of California
LOS ALAMOS, NEW MEXICO 87544

An Affirmative Action/Equal Opportunity Employer

MASTER

DISTRIBUTION OF THIS DOCUMENT IS UNLIMITED

Form No. 836
St. No. 2629
1/75

UNITED STATES
ENERGY RESEARCH AND
DEVELOPMENT ADMINISTRATION
CONTRACT W-7405-ENG. 36

DISCLAIMER

Submitted version

AN INVESTIGATION OF CREEP INSTABILITY AS A MECHANISM FOR GLACIER SURGES

W.S.B. Paterson
Polar Continental Shelf Project
Dept. of Energy, Mines & Resources
Ottawa K1A 0E4, Canada

U. Nitsan
~~Geosciences Group~~ Geological Research
University of California
Los Alamos Scientific Laboratory
Los Alamos, New Mexico 87545
U.S.A.

G.K.C. Clarke
Department of Geophysics & Astronomy
University of British Columbia
Vancouver V6T 1W5, Canada

ABSTRACT

Creep instability, the runaway increase of internal temperature and deformation rate, has been suggested as a possible cause of surges of cold glaciers. We investigate this by considering a simple slab model which includes the effect of ice advection normal to the surface. Whether a steady-state solution of the heat transfer equation exists depends on the value of a "stability parameter" proportional to the ratio of the rate of deformational heat production to the rate at which this heat is conducted away. If the parameter exceeds a certain critical value, instability occurs and basal ice eventually reaches melting point. The ice mass can then start to slide over its bed. If the stability parameter exceeds a second higher critical value, a layer of basal ice at melting point will form. The critical values depend on geothermal heat flux and strongly on advection. Upward advection, as in the ablation area, decreases stability whereas downward advection (accumulation) increases it. On the other hand, if unstable conditions exist, accumulation increases the growth rate of the instability while ablation decreases it. Calculations suggest that certain natural ice masses may be unstable. The time for the instability to develop, however, is of the order of 100 to 10,000 yr., whereas the residence time of the ice in many glaciers is less than 10,000 yr. Moreover, observed periodicities of glacier surges are between 10 and 100 yr. It thus appears that creep instability cannot explain glacier surges. These arguments do not, however, eliminate the possibility of creep instability causing surges in the Antarctic

ice sheet or in large ice-age ice sheets with low accumulation rates.

INTRODUCTION

The deformation rate of ice, for a fixed stress, increases with temperature. Thus a small increase in deformation rate, by increasing the deformational heating and thus the temperature, will result in a further increase in deformation rate. This system has positive feedback and, under certain conditions, a runaway increase in temperature will result. This is the process of creep instability. In a glacier frozen to its bed this process might in time raise the basal ice to melting point. The ice would then start to slide over its bed, lubricated by meltwater, thus changing the glaciers' velocity and dimensions.

Robin (1955) was the first to suggest this as a possible mechanism of glacier surges; he did not, however, investigate the conditions under which it might occur. Stability criteria have been derived for (a) a thick isothermal slab under constant stress (Nye, 1971), (b) laminar flow under a power flow law in a slab of finite thickness with base at the melting point (Neave and Savage, 1970), and (c) as case (b) except that the base is below the melting point (Bozhinskiy and Grigoryan, 1974; Bozhinskiy, 1975). Lliboutry (1964, p. 417) and Budd (1969) have also studied thermal instability in ice sheets.

In this paper we make a further theoretical analysis of creep instability as a possible mechanism of glacier surges. The main differences between our analysis and those of previous workers are (a) inclusion of the effect of vertical advection, an important means of heat transfer, and (b) use of the Arrhenius relation for the temperature dependence of the flow law of ice rather than an approximation to it (Frank-Kamenetzky, 1939). We have recently made a general analysis of strain heating and creep instability in glaciers and ice sheets (Clarke and others, 1977). This gives further details of some of the matters treated in the present paper.

BASIC EQUATIONS

The model is a parallel-sided incompressible slab of thickness h, resting on an inclined plane of slope α , and deforming under its own weight. The origin is on the surface and the y-axis normal to the surface, positive downwards. We assume

(a) Longitudinal heat transport is negligible compared with vertical

(b) Longitudinal strain rate is zero.

The heat transfer equation is then

σ = GREEK SIGMA
ε = EPSILON

$$\frac{\partial^2 T}{\partial y^2} - \frac{v}{k} \cdot \frac{\partial T}{\partial y} - \frac{1}{k} \cdot \frac{\partial T}{\partial t} = -2\,\sigma_{xy}\,\dot{\varepsilon}_{xy}/KJ \qquad (1)$$

Here T is temperature, v velocity perpendicular to surface, σ_{xy} shear stress, $\dot{\varepsilon}_{xy}$ shear strain rate, k thermal diffusivity, K thermal conductivity, and J mechanical equivalent of heat. Strain rate can be expressed in terms of stress by the flow law of ice (Nye, 1953) which in this case reduces to

$$\dot{\varepsilon}_{xy} = A \exp(-E/RT)\,\sigma_{xy}{}^{n} \qquad (2)$$

Here A and n are constants, E is the activation energy for creep, and R is the gas constant. ~~We make the further assumptions:~~

In this model, shear stress increases linearly with depth

$$\sigma_{xy} = y \ \sigma_B / h \qquad (3)$$

where the basal shear stress is

$$\sigma_B = \rho g \ h \ \sin \ \alpha_s \qquad (4)$$

ρ = GREEK RHO
α = ALPHA

with ρ the density of ice and g the gravitational acceleration. We make the further assumptions:

(c) Density ρ is constant.

(d) Vertical velocity decreases linearly with depth

$$v \ (y) = v_o \ (1 - y/h) \qquad (5)$$

Here and throughout the paper suffix o denotes the surface value. For the thickness of the slab to remain constant v_o must be equal to the accumulation rate ($v_o > 0$) or the ablation rate ($v_o < 0$). We also assume

(e) the temperature at the base is below the melting point. Thus our analysis does not apply to surges of temperate glaciers.

The boundary conditions are

$$T \ (0, \ t) = T_o \qquad (6)$$

$$\partial T(h,t)/\partial y \Big| = Q/K$$

Here Q is the geothermal heat flux. For time-dependent solutions of (1), the initial temperature distribution T(y,0) must also be specified.

We introduce dimensionless variables as follows:

θ = THETA
ξ = XI
τ = TAU

$$
\begin{array}{lll}
\text{temperature} & \theta = & E(T-T_o)/\,R\,T_o^{\,2} \\
\text{depth} & \xi = & y/h \\
\text{time} & \tau = & k\;t/h^2 \\
\text{constant} & \alpha = & E/\,RT_o \\
\text{advection parameter (Peclet number)} & \gamma = & h\,v_o\,/\,k \\
\text{stability parameter} & \beta = & \dfrac{2AEh^2\,\sigma_B^{\;n+1}\;\exp\,(-E/RT_o)}{K\;J\;RT_o^{\,2}} \\
\text{geothermal parameter} & \phi = & hEQ/K\;RT_o^{\,2}
\end{array}
\qquad (7)
$$

γ = GAMMA
β = BETA
φ = PHI

The stability parameter is proportional to the ratio between the rate of production of deformational heat and the rate at which this heat is conducted to the boundaries of the slab.

Equations (1) and (6) become

$$
\frac{\partial^2\theta}{\partial\xi^2} \;-\; \gamma(1-\xi)\,\frac{\partial\theta}{\partial\xi} \;+\; \beta\xi^{n+1}\,\exp\left[\theta/(1+\theta\alpha^{-1})\right] = \frac{\partial\theta}{\partial t} \qquad (8)
$$

with boundary conditions

$$\theta(0,\tau) = 0 \qquad (9)$$

$$\partial\theta(1,\tau)/\partial\xi = \phi$$

Appropriate values for the various physical constants are given in Table 1.

TABLE 1: Physical constants

E	Creep activation energy	6.07×10^{4} J mole^{-1}
R	Gas constant	8.314 J mole^{-1} deg^{-1}
K	Thermal conductivity	2.51 W m^{-1} deg^{-1}
k	Thermal diffusivity	1.33×10^{-6} m^{2} s^{-1}
J	Mechanical equivalent of heat	1
n	Flow law exponent	3
A	Flow law constant (n=3)	8.75×10^{-13} Pa^{-3} s^{-1}
ρ	Density	900 Kg m^{-3}
Q	Geothermal flux	4.18×10^{-2} W m^{-2}
		1 HFU

Our choice of the value of A lies in the middle range of values cited by Weertman (1973). Some experimental evidence suggests that the Arrhenius relation exp (-E/RT) breaks down between -10^{o}C and 0^{o}C (Mellor and Testa, 1969), but this has not yet been clearly established (Weertman, 1973).

STEADY STATE SOLUTION FOR CASE OF NO ADVECTION

We first consider this simplified case in which (8) reduces to

$$\frac{\partial^2 \theta}{\partial \xi^2} + \beta\ \xi^{n+1} \exp\left[\theta/(1+\theta\alpha^{-1})\right] = 0 \qquad (10)$$

with boundary conditions (9). This equation has to be solved numerically; our method is described by Clarke and others (1977). Because the equation is non-linear, multiple solutions are possible. Figure 1 is a schematic diagram that illustrates the physical situation. The solid curves represent the rate of strain heating for three different values of the stability parameter β. They have the shape shown because for large θ the exponential term tends to exp α, a constant. The broken curve represents the rate of heat conduction across the slab; it will increase indefinitely as θ_1, the dimensionless basal temperature, increases. (The dimensionless surface temperature is zero.) For a steady-state solution of (10) the two heat transfer terms must balance. Thus intersections of the broken and solid curves correspond to solutions. The number of solutions depends on the value of β. For β less than some critical value β_o* there is one (low temperature) solution, point P. For β greater than another critical value β_1* (>β_o*) there is one (high temperature) solution, point T. For $\beta_1^* > \beta > \beta_o^*$ there are three solutions.

The middle solution (R) is unstable because a small increase in temperature will increase the strain heating more than the conduction loss and the temperature will continue to rise until point S is reached. Similarly, a small decrease in temperature will start a cooling that will continue to point Q. Thus for $\beta_1^* > \beta > \beta_o^*$ the steady-state bed temperature cannot lie between Q and S.

Figure 2 is a schematic diagram of the steady-state basal temperature as a function of β. If, for a given glacier, $\beta < \beta_1^*$, the basal temperature will be represented by a point on the segment AB. Suppose now that the ice thickness or surface slope increases sufficiently to make $\beta = \beta_1^*$, the basal temperature will move to Cand then jump towards D. In fact, substitution of numerical values of the parameters appropriate to glaciers and ice sheets shows that the high temperature solutions (point D in Figure 2 and points S and T in Figure 1) invariably correspond to temperatures far above the melting point of ice. Thus, in reality, when β reaches β_1^* the temperature will rise until the ice at the bed reaches melting point. This changes the basal boundary condition, the ice will start to slide, its velocity will increase, and the dimensions of the glacier may change drastically. This is how creep instability can affect glaciers and ice sheets. Analysis of (10) with basal boundary condition θ_1 = constant (melting base) shows that if β is increased beyond β_1^* a second critical value β_2^* is eventually reached at which a layer of basal ice (of finite thickness) at melting point starts to form. In some cases of course the basal temperature will be at melting point for $\beta < \beta_1^*$ and there is then no instability.

The Frank-Kamenetzky approximation, frequently used to express the temperature dependence of the strain-heating term, consists in writing

$$E/RT = E/RT_o - E(T - T_o) / RT_o2 \qquad (11)$$

The exponential term in (10) then reduces to exp θ and the rate of strain heating is represented by the dotted curve in Figure 1. In this case (10) has two solutions, a low temperature stable one and a high temperature unstable one. ~~which is not physically realistic because it corresponds to temperatures far above the melting point of ice~~ This case has been analysed extensively, in the case of glaciers by Budd (1969), Neave and Savage (1970), Bozhinskiy and Grigoryan (1974), and Bozhinskiy (1975). It is found that there exists a single critical value of β, that depends on φ, above which there is no steady-state solution. Because the Frank-Kamenetzky approximation exaggerates the temperature dependence of the strain heating, this critical value of β is less than β_1^*. Numerical calculations show that the ratio of the two values is 0.97 for $\theta_1 = 1$, 0.8 for $\theta_1 = 3$, and 0.4 for $\theta_1 = 6$.

EFFECT OF ADVECTION

Advection merely changes the slope of the heat loss (broken) curve in Figure 1 and so it does not qualitatively change the results outlined in the previous section. The size of the change was investigated by numerical solution of the steady state heat transfer equation (8) with $\partial\theta/\partial\tau = 0$ (Clarke and others, 1977). Figure 3 presents the results: the value of β_1* for a range of values of advection parameter γ and geothermal parameter ϕ appropriate to glaciers and ice sheets. We took $\alpha = 30$. If the creep activation energy E has the value given in Table 1, $26.7 < \alpha < 33$ for natural ice masses. Varying α over this range would not change Figure 3 significantly. It is clear that advection has a very large effect on stability; it can change the value of β_1* by up to 4 orders of magnitude. Downward advection ($\gamma > 0$), as in the accumulation area, carries cold ice down from the surface and thus increases stability, that is, increases β_1*. Upward advection, as in the ablation area, increases the temperature of the ice mass and thus decreases stability.

Figure 3 also shows the values of the dimensionless basal temperature θ_1 when $\beta = \beta_1*$. The values are uniquely determined by γ and ϕ. To a rough approximation $T - T_o = 10\,\theta$, thus $\theta_1 = 6$ implies a basal temperature 60 degrees above the surface temperature. The figure shows that, in many cases, particularly with upward advection (ablation), β_1* corresponds to a basal temperature above melting point and thus creep instability cannot occur.

To use Figure 3 to determine the stability of a given ice mass, the values of T_o , v_o , h, σ_B, and Q must be known. The values of γ, ϕ, and β are calculated from equations 6. The value of β_1*, for the given γ and ϕ , is determined from Figure 3. The ice mass is stable or unstable according as β is less than or greater than β_1*. Table 2 shows some examples. Data sources are Budd and others (1971), Weertman (1968), and Paterson (1972). It appears that many natural ice masses may be close to instability. However, these calculations are subject to certain limitations:

(a) They are based on a theoretical model which rests on certain assumptions that may not be valid. Moreover, the model is a purely thermal one; ice dynamics is ignored.

(b) We have used numerical values of the flow law parameters and creep activation energy which are subject to considerable uncertainty.

(c) Basal shear stress and geothermal heat flux are seldom known precisely. Uncertainties in σ_B are particularly serious because β is proportional to $\sigma_B{}^4$.

TIME CONSTANTS

A further important question is: How long does the instability take to develop? If this time exceeds the residence time of ice in the particular glacier or ice sheet, the instability is of no practical importance. Again, if creep instability is a cause of glacier surges, the build-up time must correspond to the observed interval between surges.

To examine this question a steady-state solution of (8), with boundary conditions (9), was first obtained for a given set of the parameters β, γ and ϕ. The value of β was chosen to be just below critical ($\beta = 0.98\ \beta_1^*$). This solution was then used as initial condition, the value of β was increased to $1.5\ \beta_1^*$, and the time-dependent solution examined by a finite difference method (Clarke and others, 1977). Figures 4 and 5 show the temperature distribution as a function of time after the step change in β for accumulation and ablation areas ($\gamma = \pm 8$). These curves are for the special case $\phi = 0$; this explains why ~~$\partial\theta_1/\partial\xi = 0$~~ the basal temperature gradient is zero. The temperature increases with time, and at an increasing rate. At a certain time ($0.13\ \tau$ and $6.3\ \tau$ in these examples) the basal temperature starts to increase extremely rapidly; this can be regarded as the time constant of the instability. The characteristic time for thermal diffusion through a slab is h^2/k, or one unit of dimensionless time $\tau = 1$. This is the order of magnitude of the time for an instability to develop in the absence of advection. We saw earlier that, in comparison with the case of no advection, downward advection (accumulation) decreases the chance of instability. However, Figure 4 shows that, if instability does occur in the accumulation area, it develops more quickly than it would in the absence of advection. This is because downward advection compresses any layer in which instability is developing. This concentrates heat in the layer so that thermal feedback proceeds more rapidly and the time constant is reduced. Upward advection (ablation), on the other hand, stretches the layer, disperses the heat and increases the time constant, as Figure 5 shows.

The thermal regime of an ice mass may change in various ways. For example, surface temperature may change (changing ϕ, β, α), ice thickness may change (changing ϕ, β, γ), basal shear stress may change (changing β), or mass balance may change (changing γ). We consider that changes in β are the most interesting because the effect of a change in this variable is instantaneously transmitted throughout the thickness of the slab. We therefore concentrated our analysis on perturbations in β and calculated time constants for an appropriate range of values of γ and ϕ. We found that, for a given fractional step change in β, the time constant was virtually independent of ϕ, which is an important simplification. The factors that favour rapid growth of instability are strong downward advection and a large increase in β / β_1^*.

Table 3 shows the actual times for instability to develop for the unstable or marginally stable cases in Table 2. The thickness of the ice mass, assumed to be marginally stable initially, is assumed to increase by the amount shown. This increases β and makes the ice mass unstable. The quantity t_o is the order of time for the instability to develop that is, for the basal ice to reach melting point. Time constants are of the order of 100 yr for glacier accumulation areas and between 1000 and 10,000 yr for ablation areas. The latter times exceed the residence time of the ice in many glacier ablation areas. Moreover, the common interval between surges of glaciers is 10 to 100 yr. It appears impossible to get time constants as short as this in the ablation area. To obtain such time constants in the accumulation area requires accumulation rates that are relatively large for cold glaciers, combined with relatively large changes in ice thickness or basal shear stress. We therefore conclude that creep instability is not the cause of surges of cold glaciers. Actual surge periodicities for large ice sheets, if in fact they surge at all, are unknown but are certain to be much lenger than for glaciers. Thus we do not rule out the possibility that creep instability can cause ice sheets to surge.

DATA FOR REAL ICE MASSES

Table 4 contains data for some real ice masses to show the range of values of the various parameters encountered in practice. Data sources are Gow and others (1968), Budd and others (1976), Holdsworth and Bull (1970), Bull and Carnein (1970), Dansgaard and others (1973), Weertman (1968), Hattersley-Smith and others (1969), Müller (1963a, b, 1976), Redpath (1965), S.G. Collins (unpublished data), B.B. Narod and G.K.C.Clarke (unpublished data), Paterson (1968, 1976), R.M. Koerner (unpublished data), J.R. Weber (unpublished data), Weber and Andrieux (1970). Where the geothermal heat flux is unknown the world-wide average value of 1.2 H.F.U. was used. (1 H.F.U. = $4 \cdot 18 \times 10^{-2}$ .W m^{-2}.)

The calculations show that if the ice sheet at Byrd Station is near a steady-state, the basal ice must be at melting point, a fact confirmed by observation (Gow and others, 1968). If the surface temperature were lowered enough to bring the basal ice below melting point, instability would tend to develop. On the other hand, Station Crête and Camp Century in Greenland are both strongly stable with a frozen bed as a result of the greater downward advection there. Three representative ice caps in arctic Canada appear to be stable. The three glaciers chosen all appear to be melting at the bed in their ablation areas. In the case of White Glacier this is confirmed by temperature measurements (Müller, 1976). As Otto and Hazard

Glaciers are surging glaciers whereas White Glacier is not, these calculations seem to provide no basis for distinguishing surging glaciers from others. This appears to confirm the conclusion that creep instability is not the cause of glacier surges.

EFFECT OF CHANGE IN VALUE OF ACTIVATION ENERGY

In the conference discussion the question was raised as to how sensitive the results were to the value chosen for the creep activation energy E. It was even suggested that, because the Arrhenius relation with constant E does not represent the temperature dependence of the flow law near the melting point (Mellor and Testa, 1969) that relation should be abandoned. We do not consider that the experimental evidence at present available justifies abandoning the Arrhenius relation. We did however examine the effect on the time constant of changing the activation energy. Changing E changes the values of α and ϕ and thus also β_1*. Moreover, a change in E has a large effect on the value of β. The value of β/β_1*, and thus the apparent stability, is therefore changed.

An analysis that is perhaps more realistic is to keep the value of β/β_1* constant and find how much a change in E affects the time constant. Table 5 presents the results of such a test. The values of E (54 and 133 k J /mole) represent the lower and upper limits of suggested values. The low value was obtained by Paterson (1977) from analysis of borehole closure rates in the temperature range -16 to -28°C. The high value is that of Glen's (1955) laboratory experiments at temperatures between 0 and -13°C. In this test, two values of advection parameter γ and two values of geothermal heat flux Q were used . T_o was taken as 250°K, and β/β_1* was kept constant at 1.1. Table 5 shows that a change in E changes the time constant τ_o by not more than 30 %.

ACKNOWLEDGEMENTS

This work was supported by grants from the National Research Council of Canada, Environment Canada, the University of British Columbia Committee on Arctic and Alpine Research and by U.S. National Science Foundation ~~grant GA-12850~~. It was also supported by the Committee on Experimental Geology and Geophysics at Harvard University and by Div. of Physical Research, U.S. E.R.D.A., Los Alamos Scientific Laboratory, Los Alamos, New Mexico.

REFERENCES

Bozhinskiy, A.N. and Grigoryan, S.S. 1974. Possible displacement mechanism in cold glaciers. Academy of Sciences of U.S.S.R., Data on Glaciological Research, Vol. 24, p. 64-68.

Bozhinskiy, A.N. 1975. On unstable internal heating of glaciers. Isvestia Akademy Nauk U.S.S.R., Mechanics of Liquid and Gas, Vol. 5, p. 169-172.

Budd, W. 1969. The dynamics of ice masses. A.N.A.R.E. Scientific Reports, Publication 108, 216 pp. Antarctic Division, Department of Supply, Melbourne, Australia.

Budd, W.F., Jenssen, D. and Radok, U. 1971. Derived physical characteristics of the Antarctic Ice Sheet. A.N.A.R.E. Scientific Reports, Publication 120, 178 pp. Antarctic Division, Department of Supply, Melbourne, Australia.

Budd, W.F., Young, N.W. and Austin, C.R. 1976. Measured and computed temperature distributions in the Law Dome ice cap, Antarctica. Journal of Glaciology, Vol. 16, No. 74, p. 99-110.

Bull, C. and Carnein, C.R. 1970. The mass balance of a cold glacier: Meserve Glacier, South Victoria Land, Antarctica. International Association of Scientific Hydrology, Publication 86, p. 429-446.

Clarke, G.K.C., Nitsan, U. and Paterson, W.S.B. 1977. Strain heating and creep instability in glaciers and ice sheets. Reviews of Geophysics and Space Physics, Vol. 15, No. 2, in press.

Dansgaard, W., Johnsen, S.J., Clausen, H.B. and Gundestrup, N. 1973. Stable isotope glaciology. Meddelelser om Grønland, Vol. 197, p. 1-53.

Frank-Kamenetzky, D.A. 1939. Calculation of thermal explosion limits. Acta Physicochimica U.R.S.S., Vol. 10, p. 365-370.

Glen, J.W. 1955. The creep of polycrystalline ice. Proceedings of Royal Society of London, Series A, Vol. 228, No. 1175, p. 519-538.

Gow, A.J., Ueda, H.T. and Garfield, D.E. 1968. Antarctic ice sheet: preliminary results of first core hole to bedrock. Science, Vol. 161, No. 3845, p. 1011-1013.

Hattersley-Smith, G., Fuzesy, A. and Evans S. 1969. Glacier depths in northern Ellesmere Island: airborne radio echo sounding in 1966. D.R.E.O. Technical Note 69-6, 23 pp. Department of National Defence, Ottawa, Canada.

Holdsworth, G. and Bull, C. 1970. The flow law of cold ice; investigations on Meserve Glacier, Antarctica. International Association of Scientific Hydrology, Publication 86, p. 204-228.

Lliboutry, L. 1964. Traité de Glaciologie, Tome 1, 427 pp. Masson et Cie, Paris, France.

Mellor, M. and Testa, R. 1969. Effect of temperature on the creep of ice. Journal of Glaciology, Vol. 8, No. 52, p. 131-145.

Müller, F. 1963a. Accumulation studies. Axel Heiberg Island Research Reports, Preliminary Report 1961-62. p. 7-25. McGill University, Montreal, Canada.

Müller, F. 1963b. Ablation measurements in 1962. Axel Heiberg Island Research Reports, Preliminary Report 1961-62. p. 37-46. McGill University, Montreal, Canada.

Müller, F. 1976. On the thermal regime of a high-arctic valley glacier. Journal of Glaciology, Vol. 16, No. 74, p. 119-133.

Neave, K.C. and Savage, J.C. 1970. Icequakes on the Athabasca Glacier, Journal of Geophysical Research, Vol. 75, No. 8, p. 1351-1362.

Nye, J.F. 1953. The flow law of ice from measurements in glacier tunnels, laboratory experiments and the Jungfraufirn borehole experiment. Proceedings of Royal Society of London, Series A, Vol. 219, No. 1139, p. 477-489.

Nye, J.F. 1971. Causes and mechanics of glacier surges: discussion. Canadian Journal of Earth Sciences, Vol. 8, No. 2, p. 306-307.

Paterson, W.S.B. 1968. A temperature profile through the Meighen Ice Cap, arctic Canada. International Association of Scientific Hydrology, Publication 79, p. 440-449.

Paterson, W.S.B. 1972. Laurentide Ice Sheet: estimated volumes during late Wisconsin. Reviews of Geophysics and Space Physics, Vol. 10, No. 4, p. 885-917.

Paterson, W.S.B. 1976. Vertical strain-rate measurements in an arctic ice cap and deductions from them. Journal of Glaciology, Vol. 17, No. 75, p. 3-12.

Paterson, W.S.B. 1977. Secondary and tertiary creep of glacier ice as measured by borehole closure rates. Reviews of Geophysics and Space Physics, Vol. 15, No. 1, in press.

Redpath, B.B. 1965. Seismic investigations of glaciers on Axel Heiberg Island. Axel Heiberg Island Research Reports, Geophysics 1. 26 pp. McGill University, Montreal, Canada.

Robin, G. de Q. 1955. Ice movement and temperature distribution in glaciers and ice sheets. Journal of Glaciology, Vol. 2, No. 18, p. 523-532.

Weber, J.R. and Andrieux, P. 1970. Radar soundings on the Penny Ice Cap, Baffin Island. Journal of Glaciology, Vol. 9, No. 55, p. 49-54.

Weertman, J. 1968. Comparison between measured and theoretical temperature profiles of the Camp Century, Greenland, borehole. Journal of Geophysical Research, Vol. 73, No. 8, p. 2691-2700.

Weertman, J. 1973. Creep of ice. In Physics and Chemistry of Ice, edited by E. Whalley, S.J. Jones and L.W. Gold, p. 320-337. Royal Society of Canada, Ottawa, Canada.

TABLE 2. Results of stability calculations for glaciers and ice sheets.

Location	h (m)	v_o (m/yr)	T_o (°K)	σ_B (10^5 Pa)	Q (H.F.U.*)	Stability
East Antarctica, central	3000	+ 0.03	218	0.5	1.35	marginal
Antarctica, coast	1500	+ 0.5	253	1	1.5	marginal
Camp Century	1387	+ 0.35	249	0.5	1.1	stable
Laurentide Ice Sheet	3500	+ 0.3	253	0.5	1.0	stable
Laurentide Ice Sheet	3500	+ 0.3	253	1	1.0	unstable
Glacier, accumulation	300	+ 0.5	263	1	1.0	stable
Glacier, accumulation	300	+ 0.5	263	2	1.0	unstable
Glacier, accumulation	600	+ 0.25	263	1	1.0	marginal
Glacier, ablation	300	- 0.25	263	1	1.0	stable
Glacier, ablation	300	- 0.5	263	1	1.0	unstable

* 1 H.F.U. = 4.18×10^{-2} W m^{-2}

TABLE 3. Time constants for glacier and ice sheet instability.

Location	h (m)	Δh (m)	v_o (m/yr)	t_o (yr)
East Antarctica, central	3000	300	+ 0.03	50,000
Antarctica, coast	1500	150	+ 0.5	15,000
Laurentide	3500	350	+ 0.3	18,000
Glacier, accumulation	300	50	+ 1.5	90
Glacier, accumulation	300	50	+ 0.5	270
Glacier, ablation	300	50	- 0.5	1,100
Glacier, ablation	300	50	- 1.5	10,000

TABLE 4. Stability calculations for some natural ice masses.

Location	h (m)	v_o (m/yr)	T_o °K	σ_B 10^5 Pa	Q H.F.U.	β	γ	α	φ	β_1*	Remarks
Antarctica											
Byrd Station	2164	+ 0.15	245	0.6	1.85	0.585	+7.71	29.8	8.12	0.568	melting base
Law Dome, 74 Hole	390	+ 0.11	261	0.8	1.2	0.329	+1.02	28.0	0.84	1.71	stable
Meserve Gl., tunnel	30	- 0.34	254	0.7	1.2	5.6 x10⁻⁴	-0.24	28.8	0.068	2.22	stable
Greenland											
Crête	3200	+ 0.27	243	0.2	1.0	0.013	+20.5	30.1	6.60	4.08	stable
Camp Century	1387	+ 0.35	249	0.5	1.1	0.181	+11.5	29.3	3.00	4.14	stable
Canada											
Otto G.* 1000 m	700	0	255	0.7	1.2	0.337	0	28.6	1.57	0.732	stable
Otto G.* 450 m	340	- 0.80	258	0.9	1.2	0.296	-6.46	28.3	0.75	0.025	melting base
White G., "Beaver"	280	+ 0.19	263	0.6	1.2	0.065	+1.26	27.8	0.59	2.12	stable
White G., "Moraine"	300	- 0.80	257	1.9	1.2	4.13	-5.70	28.4	0.66	0.073	melting base
White G., "Anniversary"	220	- 2.00	261	1.2	1.2	0.53	-10.5	28.0	0.47	1.6 x10⁻⁴	melting base

TABLE 4. continued

Location	h (m)	v_o (m/yr)	T_o ^oK	σ_B 10^5 Pa	Q H.F.U.	β	γ	α	φ	β_1^*	Remarks
Canada											
Hazard G.*, 2300 m	180	- 1.0	267	0.7	1.2	0.074	-4.28	27.4	0.37	0.408	melting base
Hazard G.*, 2250 m	132	-1.5	267	1.0	1.2	0.165	-4.71	27.4	0.27	0.411	melting base
Hazard G.*, 2150 m	140	-2.0	267	0.1	1.2	7.6 x 10^{-6}	-6.65	27.4	0.29	0.123	melting base
Meighen Ice Cap	121	0	255.5	0.2	1.2	7.1 x 10^{-5}	0	28.6	0.27	1.98	stable
Devon Ice Cap, bore-hole	300	+0.24	250	0.6	1.2	0.020	+1.71	29.2	0.70	2.18	stable
Devon, Ice Cap Station	375	+0.12	255	1.2	1.2	0.84	+1.07	28.6	0.84	1.72	stable
Devon, S.E. 1500 m	650	+0.33	253	1.1	1.2	1.44	+5.10	28.9	1.48	2.90	stable
Penny Ice Cap	500	+0.54	260	1.1	1.2	1.75	+6.42	28.1	1.08	4.08	stable

* surging glacier

TABLE 5. Effect of change in activation energy E on time constant τ_o.

E(kJ/mole)	γ	ϕ	β_1^*	τ_o
54	11.88	1.73	5.88	0.61
133	11.88	4.27	2.87	0.54
54	0	1.73	0.665	3.38
133	0	4.27	0.076	3.10
54	11.88	3.46	3.89	0.58
133	11.88	8.53	0.918	0.44
54	0	3.46	0.203	3.29
133	0	8.53	0.003	2.73

FIGURE CAPTIONS

1. Schematic illustration of solutions of equation (10). Solid curves show how the rate of strain heating depends on basal temperature for different values of β. Dashed curve shows the rate at which this heat is lost by conduction. Intersections of these curves represent solutions of (10). Solution R is unstable; all others are stable but the high-temperature solutions S and T are not physically realistic. Dotted curve shows rate of strain heating using the Frank-Kamenetzky approximation; the intersections represent one stable and one unstable ~~(and unrealistic)~~ solution.

2. Schematic solution of equation (10) for small ϕ. As β increases the basal temperature increases along the path AB. At point C, corresponding to the critical value β_1^*, the basal temperature increases discontinuously.

3. Critical values of stability parameter β_1^* for various values of advection parameter γ and of geothermal parameter ϕ and for $\alpha = 30$. Values of dimensionless basal temperature θ_1 at onset of instability are also shown.

4. Dimensionless temperature profile as a function of dimensionless time τ after an increase in β from 0.98 β_1^* to 1.5 β_1^* for $\phi = 0$ and $\gamma = 8$ (accumulation)(left-hand and bottom axes). Dimensionless basal temperature θ_1 is also shown as a function of τ' (right-hand and top axes).

5. Dimensionless temperature profile as a function of dimensionless time τ after an increase in β from $0.98\ \beta_1$* to $1.5\ \beta_1$* for $\phi = 0$ and $\gamma = -8$ (ablation)(left-hand and bottom axes). Dimensionless basal temperature θ_1, is also shown as a function of τ (right-hand and top axes).

Paterson & others Fig 1

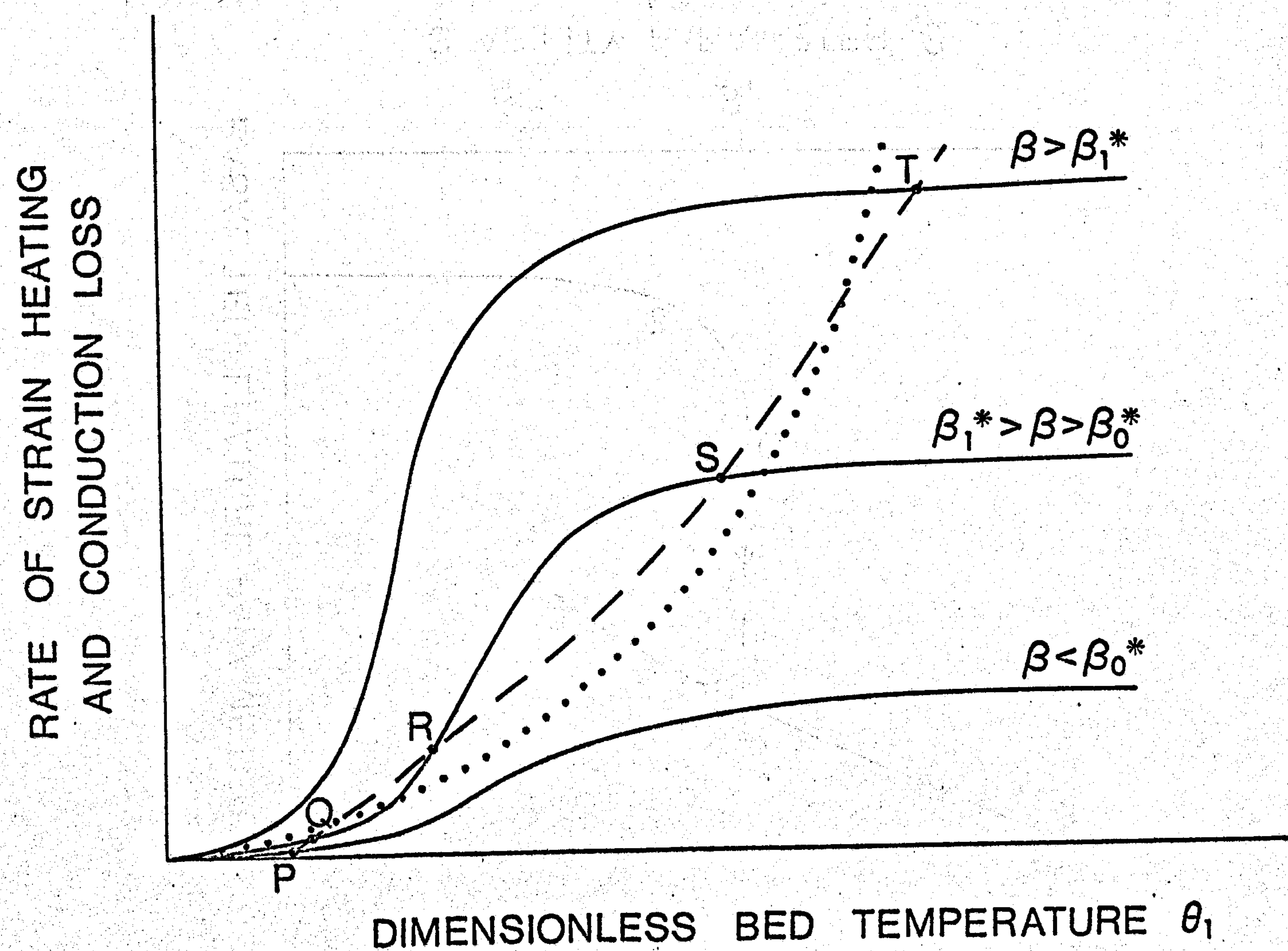

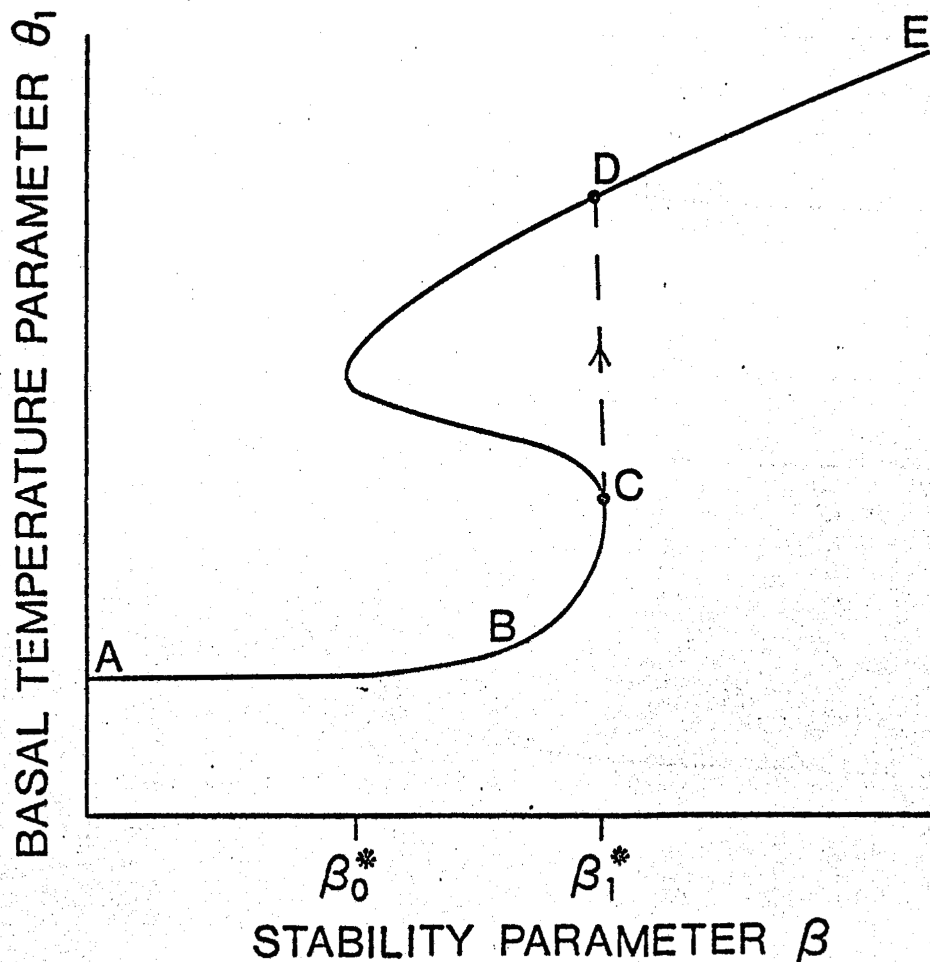
BASAL TEMPERATURE PARAMETER θ_1
A
B
C
D
E
β_0^*
β_1^*
STABILITY PARAMETER β

Paterson & others Fig. 3

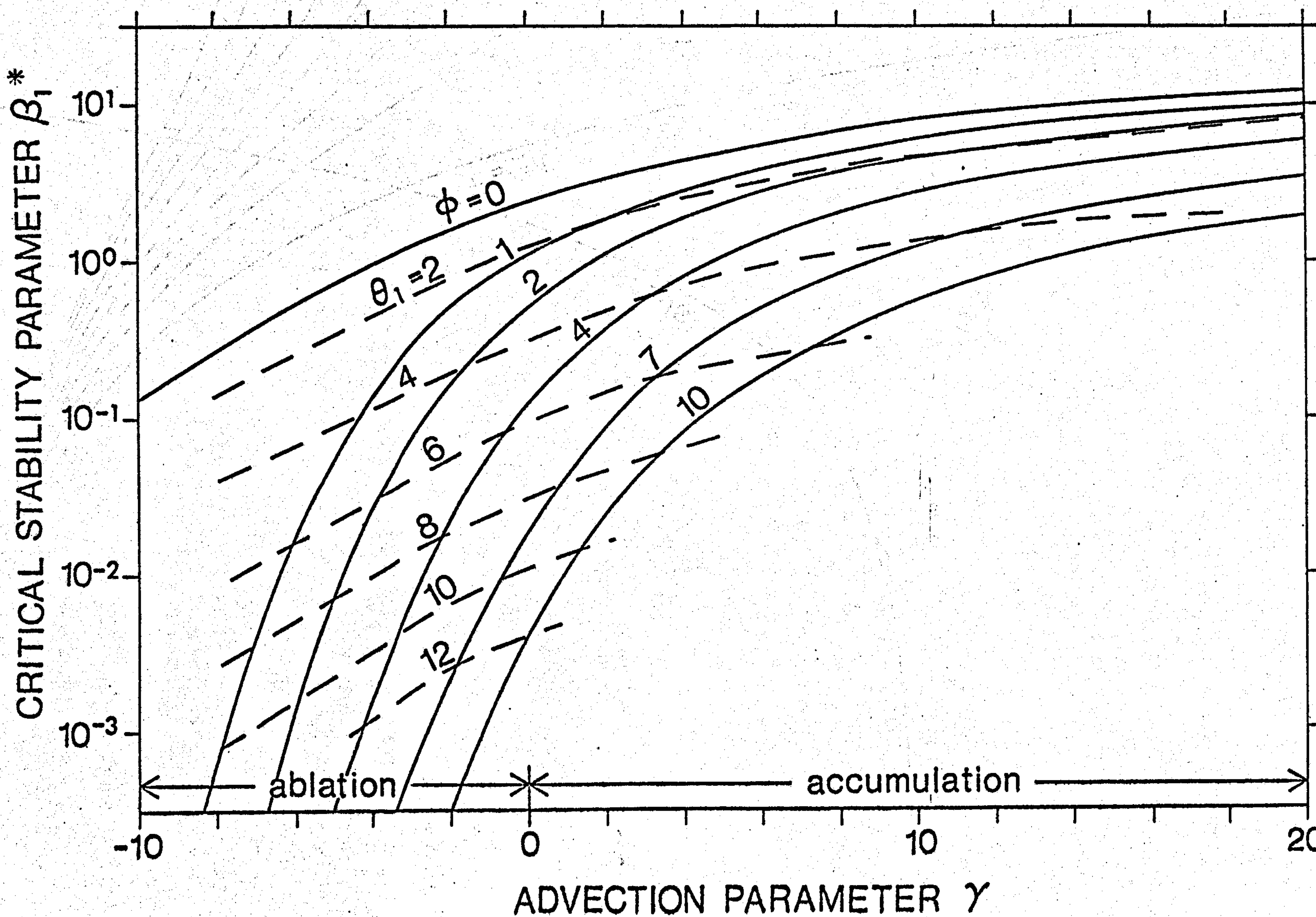

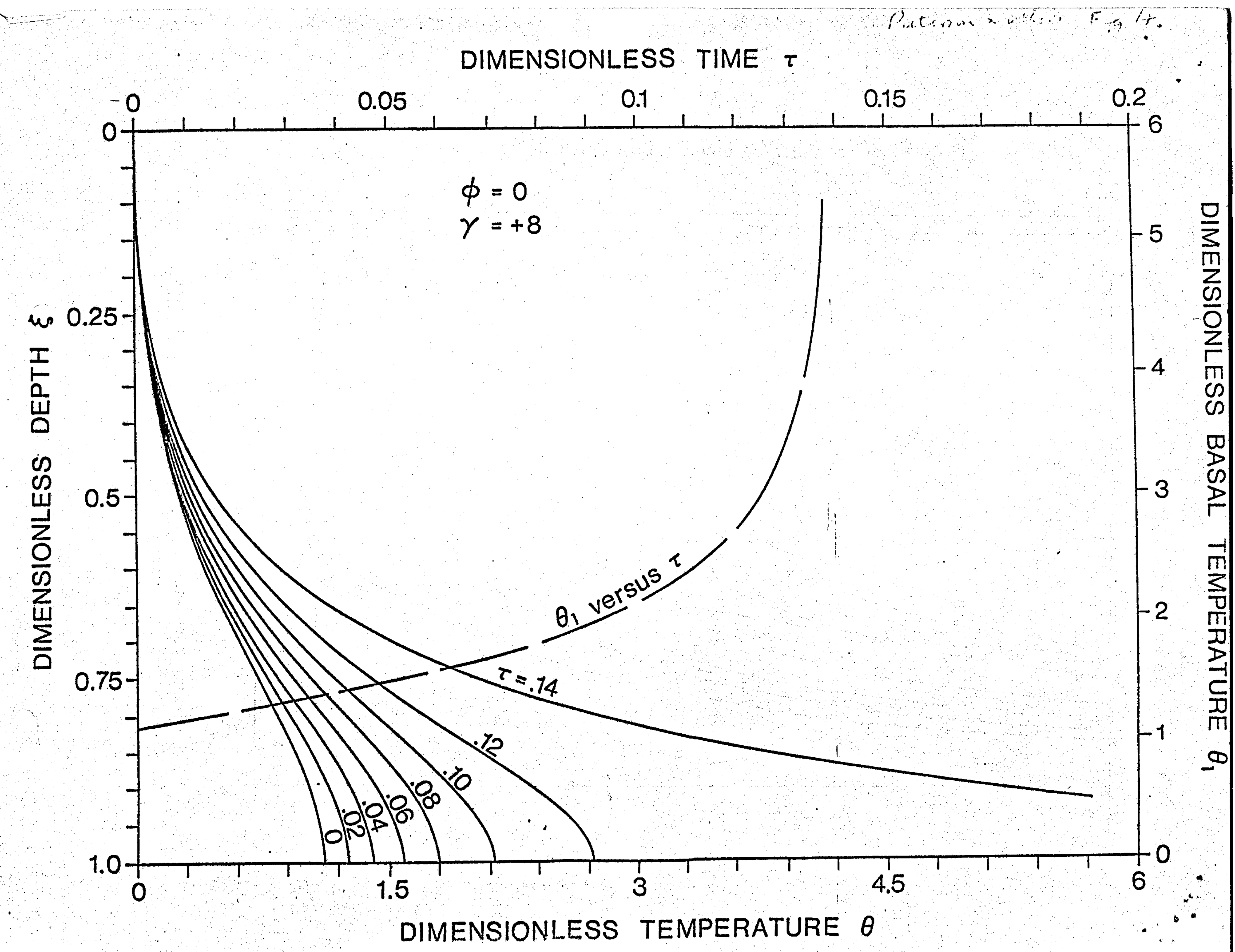

Patton & others Fig 4.
DIMENSIONLESS TIME τ
0
0.05
0.1
0.15
0.2
0
0.25
0.5
0.75
1.0
DIMENSIONLESS DEPTH ξ
6
5
4
3
2
1
0
DIMENSIONLESS BASAL TEMPERATURE θ1
φ = 0
γ = +8
θ1 versus τ
τ = .14
.12
.10
.08
.06
.04
.02
0
0
1.5
3
4.5
6
DIMENSIONLESS TEMPERATURE θ

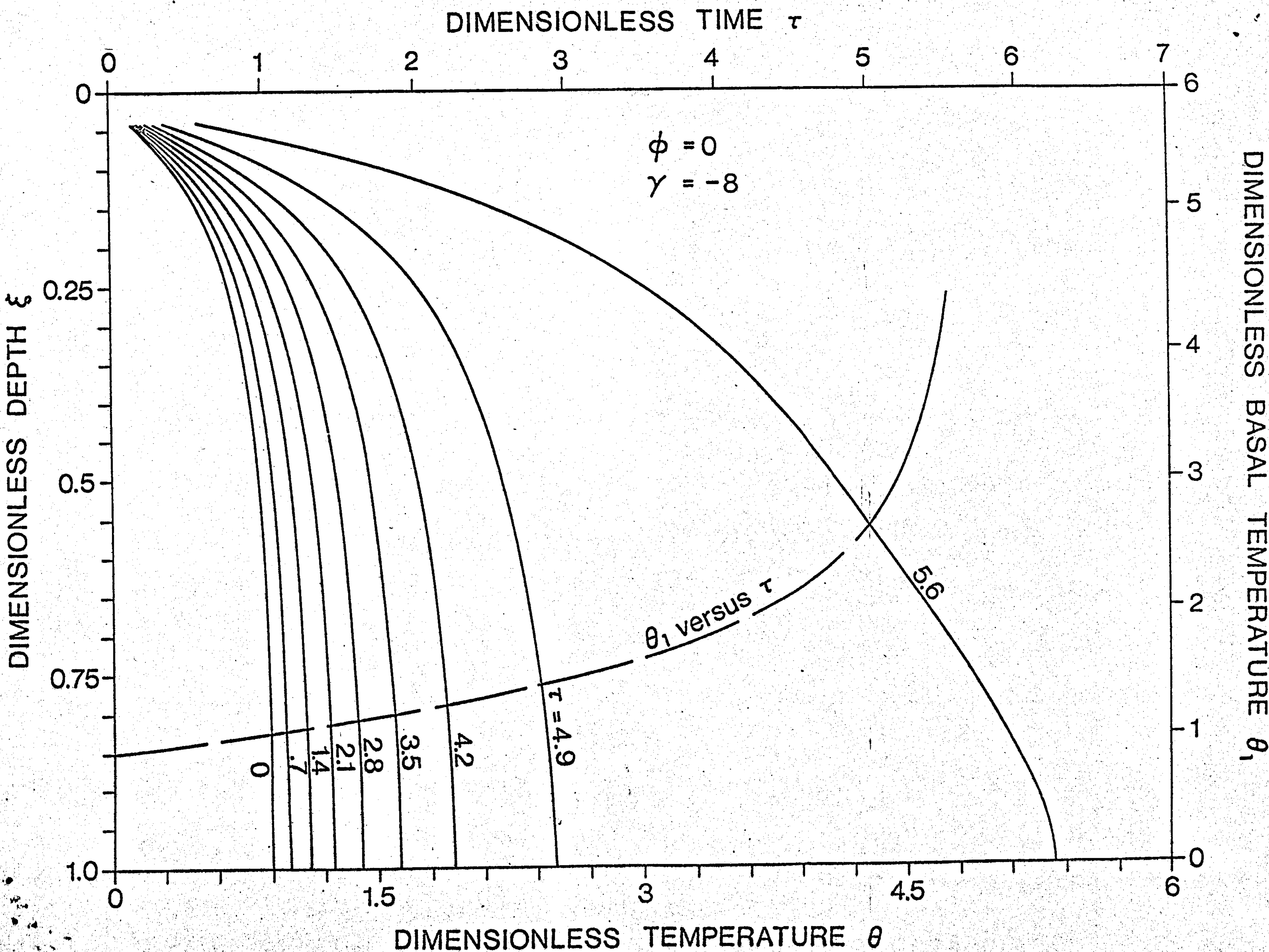
DIMENSIONLESS TIME τ
0
1
2
3
4
5
6
7
φ = 0
γ = −8
DIMENSIONLESS DEPTH ξ
0
0.25
0.5
0.75
1.0
DIMENSIONLESS BASAL TEMPERATURE θ1
6
5
4
3
2
1
0
θ1 versus τ
0
.7
1.4
2.1
2.8
3.5
4.2
τ = 4.9
5.6
DIMENSIONLESS TEMPERATURE θ
0
1.5
3
4.5
6